International Journal of Refractory Metals and Hard Materials 111 (2023) 106125

Contents lists available at ScienceDirect

International Journal of Refractory Metals and Hard Materials

journal homepage: www.elsevier.com/locate/IJRMHM

Enhancing mechanical properties of ultrafine-grained tungsten for fusion applications

Michael Wurmshuber [a,*], Simon Doppermann [a], Stefan Wurster [b], Severin Jakob [a], Mehdi Balooch [c], Markus Alfreider [a], Klemens Schmuck [a], Rishi Bodlos [d], Lorenz Romaner [a], Peter Hosemann [c], Helmut Clemens [a], Verena Maier-Kiener [a], Daniel Kiener [a]

[a] Department Materials Science, Montanuniversität Leoben, 8700 Leoben, Austria
[b] Erich-Schmid Institute of Materials Science, Austrian Academy of Sciences, 8700 Leoben, Austria
[c] Department of Nuclear Engineering, University of California, Berkeley, CA 94720, USA
[d] Materials Center Leoben GmbH, 8700 Leoben, Austria

ARTICLE INFO

Keywords:
Tungsten
Ultrafine-grained
Grain boundary segregation engineering
Small-scale testing
Mechanical properties
Nuclear fusion

ABSTRACT

Tungsten, while showing many favorable properties, faces challenges in high-performance applications due to its brittle nature. One strategy to improve strength and toughness in tungsten is to refine the grain size down to the ultra-fine grained (ufg) regime. However, as the grain size is reduced, the fraction of grain boundaries that provide easy paths for crack growth increases, thereby limiting the gain in ductility. Therefore, strengthening the grain boundaries is of great importance if one wants to tap the full potential of this material. Using ab-initio calculations, potential grain boundary cohesion enhancing doping elements were identified, and doped ultra-fine grained tungsten samples were fabricated from powders and characterized extensively using small-scale testing techniques. We found that additions of boron and hafnium improve the mechanical properties of tungsten remarkably. Furthermore, an additional low-temperature heat treatment of the boron-doped sample promotes grain boundary segregation, enhancing the properties even further. Thus, in this work we provide an effective pathway of improving mechanical properties in ultra-fine grained tungsten using grain boundary segregation engineering. This opens the door for many challenging applications of ufg W in harsh environments. To further underline the potential employment of ufg W in nuclear fusion reactors, a favorable swelling behavior and mechanical property response after irradiation with helium is presented within this work.

1. Breaking the strength-ductility trade-off

Overcoming the inherent trade-off between strength and ductility has been an important research topic ever since systematic materials science arose in the 20th century. While metals in general exhibit the best combination of strength, ductility and fracture toughness of all engineering materials, even the most advanced ultra-high strength alloys still lack sufficient deformability and damage tolerance to be considered for safety relevant structural applications [1,2]. The origin of this mutual exclusivity of strength and ductility lies in the same phenomenon as to why metals show such a good combination of mechanical properties in the first place: dislocation plasticity [3]. The generation and movement of dislocations within metals allow for plastic deformation without failure, while simultaneously providing high strength through bond energy and crystal structure [4]. As most strengthening methods in metals, such as work-hardening or precipitation hardening, rely on restricting dislocation movement, this can consequently detoriate plastic deformation and ductility. Fundamentally fracture toughness relates to the bonding strength of atoms, therefore a positive correlation between strength and toughness is observed in conventional engineering materials. For metals the fracture performance is additionally increased tremendously, as stress at the crack trip is effectively dissipated through plastic deformation by dislocation generation and propagation, a phenomenon known as intrinsic toughening [2,5]. However, once significant strengthening of metals by restricting dislocations mobility takes place, the intrinsic toughening effect is concomittantly lost, resulting in low-energy fracture and atrociously low toughness values.

There exists, however, a strengthening method in metals that commonly does not detoriate ductility: grain refinement. As demonstrated by the famous Hall-Petch relationship [6,7], mechanical strength

* Corresponding author.
E-mail address: michael.wurmshuber@unileoben.ac.at (M. Wurmshuber).

https://doi.org/10.1016/j.ijrmhm.2023.106125
Received 2 October 2022; Received in revised form 21 December 2022; Accepted 16 January 2023
Available online 19 January 2023

increases continuously with decreasing grain size. While the strength increase stems again from introducing obstacles to dislocation movement to the material, in this case grain boundaries (GBs), ductility is not reduced and sometimes can even increase by grain refinement. By visualizing a larger amount of smaller grains compared to a lesser amount of large grains, it follows that the probability of encounting grains having their slip systems orientated in a beneficial way for dislocation movement is higher with smaller grain size. Additionally, stress can be transferred to neighboring grains and activate dislocation slip systems there, allowing strength increase with sufficient plastic deformation and ductility [8,9]. Especially for metals with bcc crystal structure, grain refinement has been a popular method to enhance the fracture performance as well [10,11].

Therefore, reducing the grain size of materials to nanocrystalline (nc; grain sizes below 100 nm) and ultrafine-grained (ufg; grain sizes of 100–500 nm) regimes was expected to increase strength, ductility and toughness tremendously [9]. However, the promises of enhanced overall properties by decreasing grain size were soon proven to be wrong, as is showcased in Fig. 1. It is found that strength indeed increases remarkably upon grain refinement up until grain sizes of 10–30 nm, where an inverse Hall-Petch effect sets in [8,12]. Ductility and fracture toughness, however, start deteriorating around grain sizes of 100–200 nm and show remarkably poor values for nc grain sizes. The drop in ductility can be explained by grains getting too small to properly deform by conventional dislocation-mediated plasticity and having to rely increasingly on GB-mediated plasticity [8,13]. Furthermore, the increased amount of GBs in nc materials provide ample of easy paths for intercrystalline crack propagation, thereby reducing the fracture toughness [10,11].

By analyzing Fig. 1, one could conclude that, to maximize damage tolerance, a low grain size in the ufg regime should be favored over the ultra-high strength but poor ductility and fracture performance of nc metals.

Since GBs are identified as the weak links in metallic structures and the limiting factor to improving ductility and toughness in nc and ufg metals, significant research in the past decades focussed towards strengthening them. A promising approach to achieving this goal is the concept of grain boundary segregation engineering (GBSE) [14]. By controlling the segregation of certain elements at GBs in metals, mechanical properties can be improved in a variety of ways: The earliest examples of GBSE were based on avoiding segregation of embrittling impurity elements, such as S and P in Fe [15], definitely an essential step when trying to enhance the mechanical performance. In addition, the strength of GBs, or the GB cohesion, can be increased by doping them with certain elements that increase the bonding of GBs. A famous example is the addition of B in steels [16], Ni superalloys [17] and novel light-weight TiAl alloys [18]. The search and prediction of such GB cohesion enhancing elements has seen great support lately by ab-initio simulations, such as density functional theory (DFT) [14,19–21].

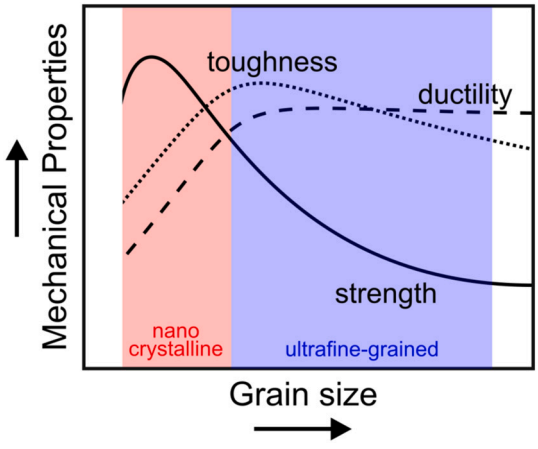

Fig. 1. Schematic trends of strength, ductility and toughness as a function of grain size in ufg and nc metals.

While the strength-ductility trade-off has been challenged in recent years with the development of TRIP and TWIP steels [22] or high-entropy alloys [23], for the ductilization of refractory metals, such as W, only limited success has been made so far. W is due to its high intrinsical strength and melting point of 3422 °C often considered for high-performance applications in harsh environments. Its excellent erosion resistance, great thermal conductivity and its low tendency to get activated or transmutate by irradiation make W especially interesting for employment in nuclear fusion reactors [24,25]. Thereby, plasma facing components, such as the divertor, experience huge amounts of radiation, thermal loads from extreme temperature fluctuations and bombardment with helium, which is known to be insoluble in metals and therefore forms gas bubbles, which can lead to blistering and other material modifications [26–32].

However, due to its high-strength nature W is known to fail in a brittle manner, either transgranular or even intergranular, already for conventional grain sizes [33–35]. As employing such a brittle material in a safety-relevant structural application is rather irresponsible, improving the mechanical properties, in particular the damage tolerance, of W is of utmost importance.

Therefore, in an effort to combine high-strength, great ductility and excellent fracture toughness in W, this work presents the fabrication of grain boundary doped ufg W via severe plastic deformation. The effect of different doping elements on strength and ductility is captured via small-scale testing methods and thoroughly discussed. Furthermore, to validate the potential application in nuclear fusion environments, the response of ufg W to helium irradiation is investigated.

2. Fabrication of ufg W

While ufg W is expected to offer improvements to overall mechanical properties and damage tolerance, its fabrication is not straightforward. Nanocrystalline W can be fabricated by desposition-based methods, such as sputtering, but the film thickness is usually limited to tens of micrometers at best. Additionally, grain sizes are usually extremely small and dislocations scarce, which results in very poor ductility and fracture toughness [9]. Therefore, when bulk ufg samples are required, grain refinement of conventionally available metals and alloys is a popular practice. While common grain refinement methods, such as rolling or forging, are limited to comparatively large grain sizes [36,37], severe plastic deformation techniques allow for smaller grain sizes and a higher percentage of more stable high-angle grain boundaries [38,39]. Due to its continuous process and the high achievable deformation strains, high pressure torsion (HPT) represents a common severe plastic deformation method. For HPT, a disk-shaped specimen is compressed under several GPa of pressure between two anvils, while one of the anvils rotates against the other. This torsional deformation leads to substantial grain refinement, while the depressions in the HPT anvils allow for sample confinement and, hence, high applied deformation strains without failure of the material. In the following, the challenges in developing a fabrication route for ufg W using HPT are described:

As the goal is to fabricate ufg W samples with certain amounts of doping elements, a powder-based fabrication approach is preferred, allowing to meticulously control the chemical composition of samples fabricated in the lab. The use of metal powders, however, harbors a high danger of surface oxidation of the powder particles. The well known oxidation risk of W powder (99.97% purity, 2 μm particle size, Plansee SE, Austria) was avoided by using a glove box filled with protective Ar gas. For transporting the powder in local Ar atmosphere outside the glove box, a small sealed mini-chamber that can be assembled inside the glovebox was utilized [40]. Cold compacting of the tungsten powder was realized using the HPT tool [41] at a nominal pressure of 12 GPa. However, as visualized in Fig. 2a, the intrinsic strength of W is too high to achieve a satisfyingly compacted microstructure. The powder

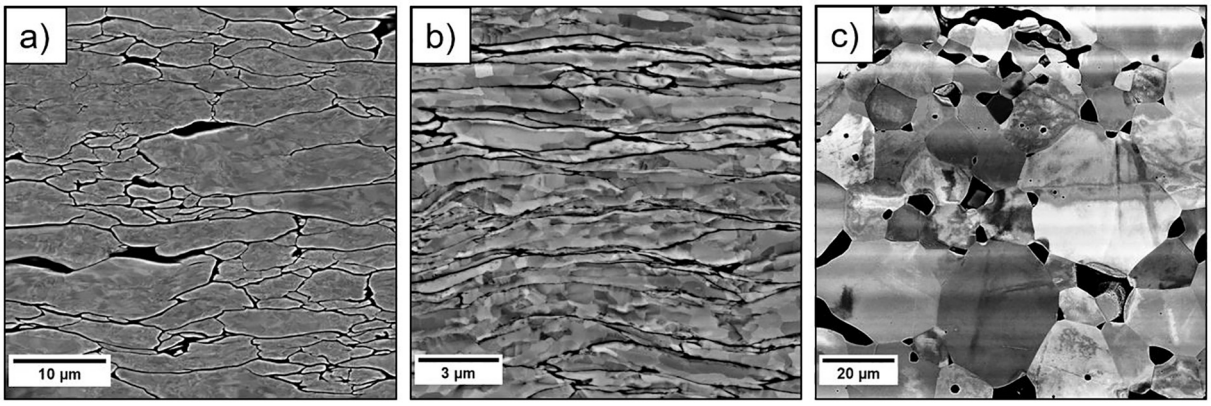

Fig. 2. SEM images of ufg W microstructures during fabrication. a) Powder compacted in the HPT. b) After HPT deformation of the compacted material. c) Compacted material after annealing at 1600 °C in vacuum. Please note that the micrographs exhibit different magnifications in order to highlight the most important respective details.

particles are clearly deformed, but sufficient interparticular bonding is lacking. Deforming such a badly compacted material in the HPT results in a vast amound of microcracks and elongated pores, as seen in Fig. 2b. Naturally, this would deteriorate ductiliy and fracture toughness of W and send us in the wrong direction on our search for strength-ductility synergy. Hence, in order to improve the interparticular connections after compacting and before HPT deformation, an intermediate heat treatment is applied. The formation and volatile nature of WO_3 oxide when annealing W in air is a well known problem in the refractory metal industry [42,43]. Therefore, all heat treatments of W materials have to be performed either under protective gas or in vacuum conditions. In this work, the compacted W samples were annealed in a vacuum furnace (Leybold Heraeus PD 1000, Leybold GmbH, Germany) at 1600 °C for 7 h.

After this annealing step, the microstructure (Fig. 2c) exhibits bonding between grains and former powder particles (i.e. no microcracks along GBs and pores only present at triple junctions). The apparent grain growth and residual porosity are not of concern, as the subsequent HPT deformation will refine the grain size and compact the microstructure even further.

After processing the powder derived bulk precursor, grain refinement via a HPT deformation is the next step. Due to its high instrinsical strength, deformation of W is a challenging task. In order for HPT to successfully deform a material, the anvil material has to be somewhat harder than the sample [41]. At room temperature this is not the case, as dislocation plasticity is not fully activated in W yet. Utilizing the built-in heating option of the HPT tool has to be done carefully, as the tool steel used for the anvils significantly loses its hardness at temperatures above

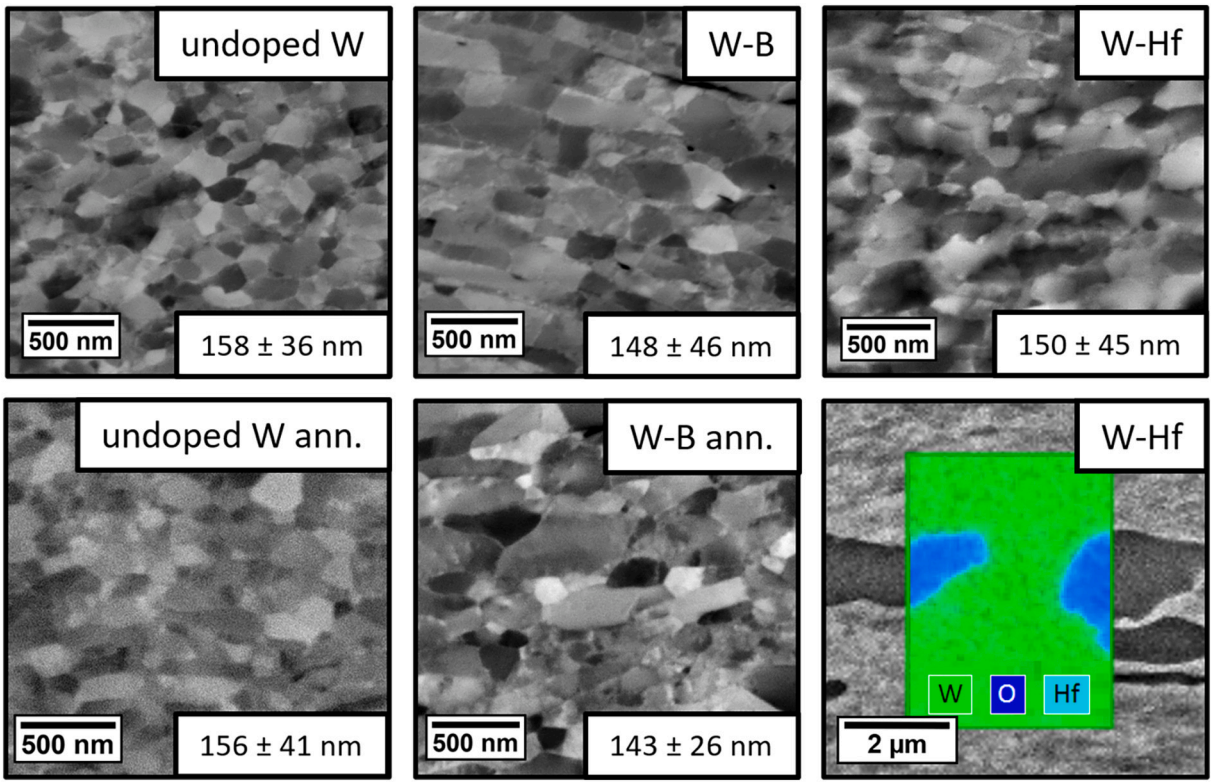

Fig. 3. SEM images of the microstructures and grain sizes, derived by line interception method of investigated doped and undoped ufg W samples fabricated by HPT. Bottom right: EDX map of HfO_2 particles in Hf-doped sample.

400 °C. Thus, there exists only a tight temperature window in which W can be deformed using HPT. We did so at 400 °C under a nominal pressure of 12 GPa for about 1 rotation. After this, the material is already too hard to be deformed further by the available anvils. Due to the torsional nature of the deformation, a microstructural gradient is present in the sample disk. The final microstructures of HPT deformed (doped and undoped) W samples at a radius of 3 mm demonstrate grain sizes of approximately 150 nm, as shown in Fig. 3.

3. Grain boundary doping of ufg W

After establishing a reliable fabrication route for ufg W starting from powder materials, mechanical property enhancements through GB doping can be realized. The selection of suitable doping elements was based on DFT calculations by Scheiber et al. [19,20]. The following elements that have favorable phase diagrams with W were chosen: B (98% purity, 44 µm particle size, Alfa Aesar, USA) and Hf (99.6% purity, 44 µm particle size, Alfa Aesar, USA). The powders were mixed with W to a content of about 3–5 at.%. Undoped and doped ufg W samples were processed via the presented fabrication route and their microstructures are shown in Fig. 3. Additionally, an undoped W and a B-doped W sample were annealed after HPT deformation at 500 °C for 5 h in vacuum. As apparent in Fig. 3, no grain growth occurred for annealed samples, indicated "ann.". Moreover, in contrast to other HPT works [44], the addition of doping elements does not seem to have an influence on the HPT deformation and resulting microstructure, most likely because none of the samples are deformed to their respective saturation grain sizes.

As weighing in such small amounts of doping elements to be mixed with W is rather challenging, the compositions of doping elements were confirmed to be about 3–5 at.% in subsequent EDX measurements.

Due to the torsional nature of the HPT process a deformation strain gradient is present in the sample disks, with the outer regions of the disk experiencing more plastic deformation than the sample center. This deformation gradient expresses itself in a microstructural and property gradient, causing the outer region of the sample disks to exhibit smaller grain size and higher hardness and strength. As the desired microstructure is only available in a small region towards the edge of the samples (in this work defined as 3 mm from the disk center), small-scale testing techniques have to be applied to investigate the effect of each doping element and the heat treatments on the mechanical properties of ufg W. In this work, microcantilever bending tests were utilized due to their straightforward fabrication and testing and their partial tensile nature, testing the most crucial loading mode for W and ufg materials in general. 3–4 cantilevers of dimensions 3x3x10 µm were fabricated for each material using pre-grinding and a FIB workstation (Zeiss LEO 1540XB, Zeiss GmbH, Germany). The cantilevers were tested in radial direction of the sample disk using an UNAT-SEM indenter (Zwick GmbH Co & KG, Germany) equipped with a conductive diamond wedge indenter tip (Synton MDP-AG, Switzerland) inside an SEM (Zeiss LEO 982, Zeiss GmbH, Germany). The recorded force-displacement data can be converted to bending stress and bending strain using the conventional formulae given in [45,46].

For comparison among all ufg W samples, the maximum bending stress was utilized as a measure for strength. For ductility, the plastic bending strain at failure was used. This failure point was identified for each tested cantilever from in-situ images and load drops in the stress-strain curve. Such a compiled "strength-ductility map" is shown in Fig. 4. To visualize the improvement in damage tolerance and the success in breaking the strength-ductility trade-off by GB doping, isolines representing the product of strength and ductility in MJ/m^3 were added to Fig. 4. In the following, the effect of annealing and each doping element is described in detail:

The considerable strength increase from the heat treatment of the undoped W sample is a phenomenon commonly observed in nanostructured metals. This hardening-by-annealing effect is usually

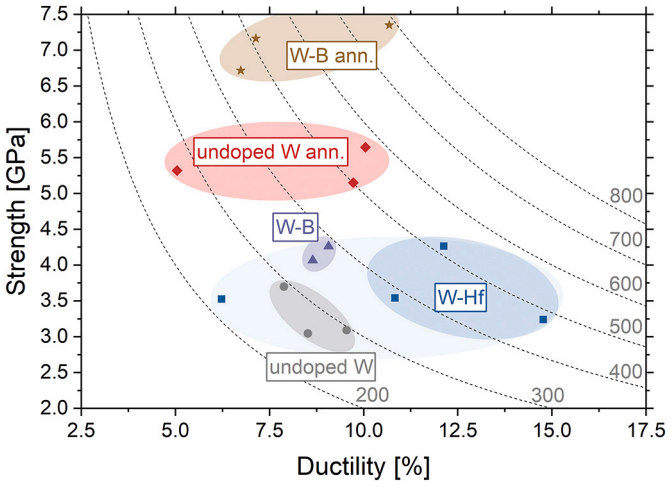

Fig. 4. a) Maximum bending stress ("strength") over plastic bending strain at failure ("ductility") for all investigated samples. Isolines represent the damage tolerance (i.e. product of strength and ductility) of the material in MJ/m^3.

attributed to annihilation of mobile dislocations at GBs and relaxation of GBs to a thermodynamically stable state [47,48]. As a consequence, plastic deformation is only possible through dislocation nucleation at relatively "smooth" GBs, i.e. GBs that do not exhibit ledges or similar defects where dislocation nucleation is facilitated [49]. Therefore a higher stress has to be applied to the material for dislocation nucleation to set in and the material to deform. The movement of such GB-nucleated dislocations through the obstacle-free grain is not restricted and, due to the small grain size, dislocations annihilate at GBs rather than piling up in front of them, which is why ductility is not affected by this annealing effect. After all, the GB cohesion is still believed to be the limiting factor to ductility in such fine grained metals. It should be noted that, in order to make use of this hardening-by-annealing effect, the heat treatment has to be conducted at temperatures below the grain growth threshold temperature.

Doping of ufg W with the interstitial element B increases the bending strength of ufg W while maintaining ductility, leading to an immense increase in damage tolerance. The GB cohesion enhancing properties of B [19], in addition to a site competition with the embrittling interstitial element O, are the reason for this improvement of mechanical properties. Therefore B strengthens the GBs of W both directly and indirectly by replacing O from the GBs. When combining the B doping of ufg W with a heat treatment, a tremendous increase in strength is observed, while ductility still remains around the same level as the undoped W sample. This enormous enhancement of strength and damage tolerance is attributed on one hand to the hardening-by-annealing effect described above, and on the other hand to the increased diffusion and segregation of B at the GB, amplifying the positive effect of B on W GBs.

The substitutional doping element Hf does not have a GB cohesion enhancing effect in W according to DFT simulations [20]. However, its affinity to O is frequently taken advantage of in engineering alloys that struggle with mechanical property degradation from O impurities. In fact, Hf has been used to improve the mechanical properties and toughness of Mo [33]. The idea is for Hf to bind O, which is commonly located at GBs and a well-known embrittling element, in HfO_2. Indeed, such HfO_2 oxides are present in the microstructure of W—Hf samples, as evidenced in Fig. 3 (bottom right). Thereby, GBs in W are strengthened indirectly, which results in an increase in strength, ductility and damage tolerance, as observed in the microcantilever bending tests (Fig. 4). One of the W—Hf samples showed no improvement of mechanical properties over the undoped W material. This might indicate that Hf is not consistently efficient in binding oxygen throughout the material.

Altogether, the mechanical properties of ufg W can be significantly

enhanced by doping with Hf and B. This enhancement can be further optimized by performing a heat treatment at temperatures below the grain growth threshold, which results in a hardening-by-annealing effect. While only Hf was successful in improving both strength and ductility of ufg W, the strength increase by B and annealing was not accompanied by a loss in ductility and therefore also improves damage tolerance and contradicts the strength-ductility trade-off. To capture the impact of doping elements on the third important mechanical property toughness, fracture mechanical investigations are planned in the future.

4. Performance of ufg W in nuclear fusion environments

It was shown that through grain refinement and systematically modifying GB chemistry the mechanical properties and damage tolerance of W can be pushed to unprecedented values. This makes an employment of W in safety relevant applications and harsh environments attractive and possible. As mentioned in the introduction, W is frequently considered for application in novel nuclear fusion reactors. Aside from the well researched irradiation, mechanical and thermal loads, an important aspect that is often overlooked in a plasma-based fusion environment is the continuous production of helium by the deuterium-tritium fusion reaction [50]. Because the noble gas He is insoluble in metals, it frequently accumulates and forms gas bubbles within the material, often in conjunction with radiation-induced vacancies. The formation and growth of He bubbles leads to swelling of the material and a serious degradation of mechanical properties, as the material is slowly transforming into a foam-like structure [51]. The nucleation and evolution of He bubbles within W of different grain sizes has been studied in recent years [27,31,52]. However, the concrete implications on swelling behavior and mechanical properties have not been captured yet and will therefore be investigated herein.

To study the performance of ufg W under helium irradiation, 25 keV He ions were implanted to fluences of 6×10^{17} ions/cm^2 and 10^{18} ions/cm^2 in 10×10 μm^2 squares on the polished surface of (undoped) ufg W (radius of 3 mm on the sample disk) using a helium-ion microscope (Zeiss Orion NanoFab, Zeiss Gmbh, Germany) [53]. The dose rate was 1 dpa/min and the penetration depth was simulated using the software "SRIM" [54] to be about 180 nm. Commonly, He ions (α-particles) produced in the deuterium-tritium fusion reaction possess a higher energy of up to 3.5 MeV [55]. However, this would only influence the penetration depth of the helium and not the overall microstructural changes in irradiated materials, as long as similar fluences are compared and the energy of the particle is higher than the displacement threshold energy of the target material (around 85 eV for tungsten [56,57]).

The target fluences were selected based on previous research works [27,29–32,58], which show that in this range of fluence significant changes to the microstructure, i.e. pronounced bubble formation and growth, blister formation, fuzz formation, etc., occur for W and other metals.

A popular method to evaluate the swelling of materials after helium implantation is atomic force microscopy (AFM) [27,51]. By utilizing a Nanoscope III AFM (Digital Instruments, USA) in tapping mode, the topologies in and around the implanted squares were investigated. The average height difference between implanted and pristine material regions is commonly referred to as "swelling height" and is a straightforward and convenient value for comparing the swelling response between different samples (see Fig. 5a). The measured swelling height values of ufg W and single-crystalline (sxx) W from Ref [27] are shown and compared in Fig. 5b. It is evident that the swelling response to all investigated fluences of He is similar for both W materials. This is rather surprising, as the large amount of GBs present in the ufg sample was expected to have some influence on swelling. In previous work, for example, it was shown that GBs can have a negative (facilitated nucleation of bubbles on GBs) or positive (restricted growth of bubbles through GBs; annihilation of vacancies before clustering to bubbles with He) effect on bubble morphology and swelling behavior [51]. It is assumed that the grain size of about 150 nm is still too large to have a noticeable impact on helium bubble formation and growth. This is supported by investigations of El-Atwani et al. [31], who identified a grain size threshold of 35–50 nm for W. Above this threshold, GBs are too widely spaced to effectively remove radiation-induced vacancies before they can cluster to bubbles with He atoms. Therefore, no impact of the GBs on the measured swelling height is observed. That being said, W, as a pure bcc metal, shows excellent swelling behavior even as single crystal material, outperforming novel nc bcc-fcc composites [51]. It seems, however, that the smaller grain size is beneficial against the formation of large blisters, as no such blisters are observed for ufg W (Fig. 5a) in AFM micrographs, while they pose a serious problem in sxx W [27]. Previous TEM works confirm that nanocrystalline and ufg metals are not prone to blistering [29,30,32,51], even at such high helium fluences, whereas coarse grained and sxx metals are [27,58]. Whenever blister formation occurred in these works, it was also clearly visible from AFM images.

The mechanical properties of irradiated materials are commonly evaluated using small-scale testing methods, due to the limited available sample volume [59,60]. This work utilizes nanoindentation (TI 950 Triboindenter, Hysitron Inc., USA) with a continuous stiffness measurement (CSM) option to probe the hardness and reduced modulus of

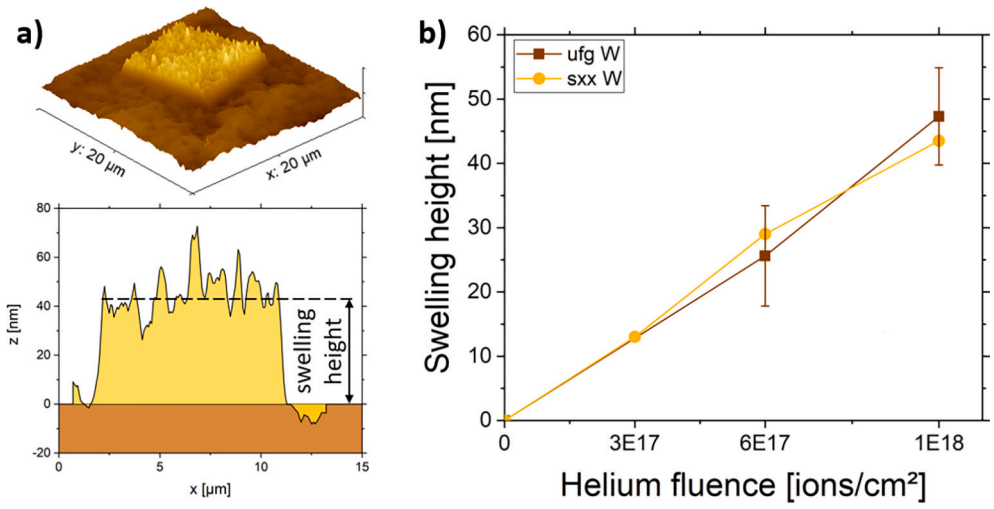

Fig. 5. Swelling measurements of helium-implanted W. a) Representative AFM micrograph of ufg W implanted with helium fluence of 10^{18} ions/cm^2 and schematic on the definition of swelling height. b) Measured swelling heights of ufg W compared to swelling of sxx W [27]. Error bars represent RMS mean roughness.

ufg W in pristine and irradiated conditions. The averaged results for each helium fluence are shown in Fig. 6. It is apparent that the reduced modulus shows a decreasing trend with increasing helium fluence. This is logical, as more and more gas is implanted into the material and it is slowly transforming into a foam-like structure. However, contrary to intuition, the hardness does not decrease after implantation with a helium fluence of 6×10^{17} ions/cm^2. Instead, the nanoindentation results suggest a constant trend of hardness up to this very respectable amount of implanted helium and only drops significantly after irradiation with an even higher fluence of 10^{18} ions/cm^2. Rather than being unaffected by the helium irradiation, the trend of a sustained hardness is explained by a competition between two effects: i) softening of the material by gas bubble formation and growth, which is predominant for higher fluences, and ii) radiation hardening through radiation-induced defects and defect clusters, a common phenomenon found in irradiated metals [51]. While these competing effects result in no apparent change in hardness for the fluence of 6×10^{17} ions/cm^2, a serious decrease in ductility and toughness can be expected.

5. Summary and conclusion

In summary, this comprehensive work has investigated the potential of enhancing the mechanical performance of W by grain refinement and grain boundary segregation engineering, in an attempt to break the strength-ductility trade-off. A reproducible and reliable fabication route for bulk ufg W with grain sizes of about 150 nm was developed and presented herein. Using this powder-based fabrication route, ufg W doped with ab-initio informed elements was fabricated and the strength and ductility were evaluated by microcantilever bending tests. A clear improvement of mechanical properties of ufg W could be achieved via doping with B and Hf, as well as through heat treatments below the grain growth threshold temperature. Although we still lack the means to produce ufg W in large quantities, these exciting enhancements in mechanical performance are expected to have significant implications on the employment of W in nuclear fusion reactors. For example, similar mechanical property enhancements are expected when applying the same doping strategies to cold-rolled W sheets, exhibiting grain sizes of 200–400 nm [36,61]. The response of ufg W to helium irradiation, a major concern in fusion environments, was also investigated within this work. While the measured swelling of ufg W shows no improvement compared to the already potent single crystal W, a suppressed blister formation was observed. Additionally, it was found that softening of ufg W through bubble formation and growth is delayed to higher doses, as a competing radiation hardening effect maintains the hardness at higher levels. In conclusion, impressive advancements in the fabrication and strengthening of W have been made within this work, rendering the material attractive for usage in high performance applications, such as novel nuclear fusion reactors.

CRediT authorship contribution statement

Michael Wurmshuber: Conceptualization, Methodology, Formal analysis, Investigation, Writing – original draft, Visualization. **Simon Doppermann:** Investigation, Formal analysis. **Stefan Wurster:** Methodology, Writing – review & editing. **Severin Jakob:** Investigation, Methodology, Formal analysis. **Mehdi Balooch:** Investigation, Formal analysis. **Markus Alfreider:** Methodology. **Klemens Schmuck:** Methodology. **Rishi Bodlos:** Methodology, Software. **Lorenz Romaner:** Conceptualization, Methodology. **Peter Hosemann:** Conceptualization, Methodology. **Helmut Clemens:** Conceptualization. **Verena Maier-Kiener:** Methodology. **Daniel Kiener:** Conceptualization, Methodology, Resources, Writing – review & editing, Supervision, Project administration, Funding acquisition.

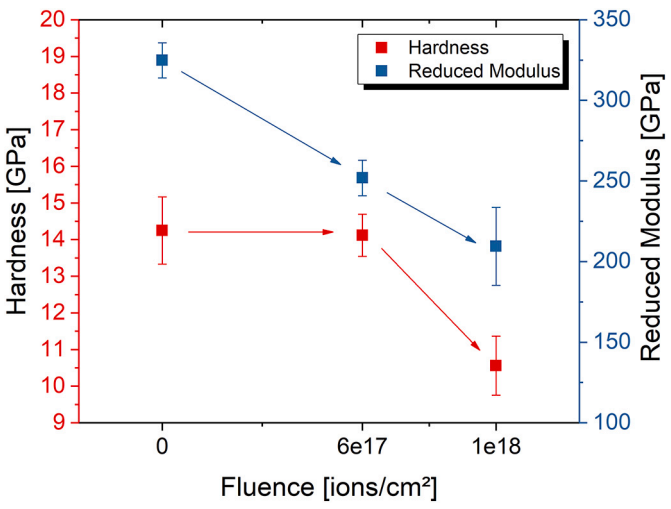

Fig. 6. Average hardness and reduced modulus of ufg W in unirradiated and irradiated conditions measured via nanoindentation.

Declaration of Competing Interest

The authors declare that they have no known competing financial interests or personal relationships that could have appeared to influence the work reported in this paper.

Data availability

Data will be made available on request.

Acknowledgements

Financial support by the European Research Council under the Horizon 2020 Act, Grant Nr. 771146 (TOUGHIT) is greatly acknowledged. The authors thank Dr. Wolfram Knabl, Dr. Judith Köstenbauer and Plansee SE for providing tungsten material powder and support with sample annealing.

References

[1] M.F. Ashby, Materials Selection in Mechanical Design, Butterworth-Heinemann, Oxford, 2011.
[2] R.O. Ritchie, Nat. Mater. 10 (2011) 817–822.
[3] B.B. He, B. Hu, H.W. Yen, G.J. Cheng, Z.K. Wang, H.W. Luo, M.X. Huang, Science (80-.) 357 (2017) 1029–1032.
[4] G. Gottstein, Physical Foundations of Materials Science, Springer, Berlin-Heidelberg, 2004.
[5] M.E. Launey, R.O. Ritchie, Adv. Mater. 21 (2009) 2103–2110.
[6] E.O. Hall, Proc. Phys. Soc. 64 (1951) 747–753.
[7] N.J. Petch, J. Iron Steel Inst. 174 (1953) 25–28.
[8] M.A. Meyers, A. Mishra, D.J. Benson, Prog. Mater. Sci. 51 (2006) 427–556.
[9] C.C. Koch, I.A. Ovidko, S. Seal, S. Veprek, Structural Nanocrystalline Materials - Fundamentals and Applications, Cambridge University Press, Cambridge, 2007.
[10] R. Pippan, A. Hohenwarter, Mater. Res. Lett. 4 (2016) 127–136.
[11] A. Hohenwarter, R. Pippan, Philos. Trans. R. Soc. A 373 (2015) 20140366.
[12] C.E. Carlton, P.J. Ferreira, Acta Mater. 55 (2007) 3749–3756.
[13] C.C. Koch, D.G. Morris, K. Lu, A. Inoue, MRS Bull. 24 (1999) 54–58.
[14] D. Raabe, M. Herbig, S. Sandlöbes, Y. Li, D. Tytko, M. Kuzmina, D. Ponge, P. Choi, Curr. Opin. Solid State Mater. Sci. 18 (2014) 253–261.
[15] P. Lejcek, Grain Boundary Segregation in Metals, Springer, Berlin-Heidelberg, 2010.
[16] R. Wu, A.J. Freeman, G.B. Olson, Science (80-.) 265 (2006) 376–380.
[17] C.T. Liu, C.L. White, J.A. Horton, Acta Metall. 33 (1985) 213–229.
[18] H. Clemens, S. Mayer, Adv. Eng. Mater. 15 (2013) 191–215.
[19] D. Scheiber, R. Pippan, P. Puschnig, L. Romaner, Model. Simul. Mater. Sci. Eng. 24 (2016) 85009.
[20] D. Scheiber, R. Pippan, P. Puschnig, A. Ruban, L. Romaner, Int. J. Refract. Met. Hard Mater. 60 (2016) 75–81.
[21] H. Lee, V. Tomar, Comput. Mater. Sci. 77 (2013) 131–138.
[22] N. Fonstein, Advanced High Strength Sheet Steels, Springer International Publishing, 2015.

[23] B. Gludovatz, A. Hohenwarter, D. Catoor, E.H. Chang, E.P. George, R.O. Ritchie, Science (80-.) 345 (2014) 1153–1158.
[24] M. Rieth, D.E.J. Armstrong, B. Dafferner, S. Heger, A. Hoffmann, M. Hoffmann, U. Jäntsch, M. Rohde, T. Scherer, V. Widak, H. Zimmermann, Adv. Sci. Technol. 73 (2010) 11–21.
[25] S. Wurster, N. Baluc, M. Battabyal, T. Crosby, J. Du, C. Garcia-Rosales, A. Hasegawa, A. Hoffmann, A. Kimura, H. Kurishita, R.J. Kurtz, H. Li, S. Noh, J. Reiser, J. Riesch, M. Rieth, W. Setyawan, M. Walter, J.-H. You, R. Pippan, J. Nucl. Mater. 442 (2013) 181–189.
[26] D.R. Olander, Fundamental Aspects of Nuclear Reactor Fuel Elements, Technical Information Center, Office of Public Affairs, Energy Research and Development Administration, Springfield, USA, 1977.
[27] F.I. Allen, P. Hosemann, M. Balooch, Scr. Mater. 178 (2020) 256–260.
[28] Z. Chen, L.L. Niu, Z. Wang, L. Tian, L. Kecskes, K. Zhu, Q. Wei, Acta Mater. 147 (2018) 100–112.
[29] O. El-Atwani, K. Hattar, J.A. Hinks, G. Greaves, S.S. Harilal, A. Hassanein, J. Nucl. Mater. 458 (2015) 216–223.
[30] O. El-Atwani, J.A. Hinks, G. Greaves, S. Gonderman, T. Qiu, M. Efe, J.P. Allain, Sci. Rep. 4 (2014) 4–10.
[31] O. El-Atwani, J.A. Hinks, G. Greaves, J.P. Allain, S.A. Maloy, Mater. Res. Lett. 5 (2017) 343–349.
[32] O. El-Atwani, S. Gonderman, M. Efe, G. De Temmerman, T. Morgan, K. Bystrov, D. Klenosky, T. Qiu, J.P. Allain, Nucl. Fusion 54 (2014).
[33] K. Leitner, D. Scheiber, S. Jakob, S. Primig, H. Clemens, E. Povoden-Karadeniz, L. Romaner, Mater. Des. 142 (2018) 36–43.
[34] B. Gludovatz, S. Wurster, A. Hoffmann, R. Pippan, Int. J. Refract. Met. Hard Mater. 28 (2010) 674–678.
[35] B. Gludovatz, S. Wurster, T. Weingartner, A. Hoffmann, R. Pippan, Philos. Mag. 91 (2011) 3006–3020.
[36] J. Reiser, J. Hoffmann, U. Jäntsch, M. Klimenkov, S. Bonk, C. Bonnekoh, A. Hoffmann, T. Mrotzek, M. Rieth, Int. J. Refract. Met. Hard Mater. 64 (2017) 261–278.
[37] S. Wurster, B. Gludovatz, A. Hoffmann, R. Pippan, J. Nucl. Mater. 413 (2011) 166–176.
[38] R.Z. Valiev, R.K. Islamgaliev, I.V. Alexandrov, Prog. Mater. Sci. 45 (2000) 103–189.
[39] R. Pippan, S. Scheriau, A. Taylor, M. Hafok, A. Hohenwarter, A. Bachmaier, Annu. Rev. Mater. Res. 40 (2010) 319–343.
[40] M. Wurmshuber, S. Doppermann, S. Wurster, D. Kiener, I.O.P. Conf, Ser. Mater. Sci. Eng. 580 (2019), 012051.
[41] R. Pippan, S. Scheriau, A. Hohenwarter, M. Hafok, Mater. Sci. Forum 584–586 (2008) 16–21.
[42] E. Lassner, W.-D. Schubert, Tungsten., Properties, Chemistry, Technology of the Element, Alloys, and Chemical Compounds, Kluwer Academic / Plenum Publishers, New York, 1999.
[43] A. Warren, A. Nylund, I. Olefjord, Int. J. Refract. Met. Hard Mater. 14 (1996) 345–353.
[44] R. Pippan, F. Wetscher, M. Hafok, A. Vorhauer, I. Sabirov, Adv. Eng. Mater. 8 (2006) 1046–1056.
[45] E. Carrera, G. Giunta, M. Petrolo, Beam Structures: Classical and Advanced Theories, John Wiley & Sons, 2011.
[46] C. Motz, T. Schöberl, R. Pippan, Acta Mater. 53 (2005) 4269–4279.
[47] X. Huang, N. Hansen, N. Tsuji, Science (80-.) 312 (2006) 249–251.
[48] O. Renk, A. Hohenwarter, K. Eder, K.S. Kormout, J.M. Cairney, R. Pippan, Scr. Mater. 95 (2015) 27–30.
[49] H. Van Swygenhoven, J.R. Weertman, Mater. Today 9 (2006) 24–31.
[50] E. Rebhan, D. Reiter, R. Weynants, U. Samm, W.J. Hogan, J. Raeder, T. Hamacher, in: K. Heinloth (Ed.), Landolt-Börnstein Numer. Data Funct. Relationships Sci. Technol. Gr. VIII Adv. Mater. Technol, Springer, 2005, pp. 304–368.
[51] M. Wurmshuber, D. Frazer, M. Balooch, I. Issa, A. Bachmaier, P. Hosemann, D. Kiener, Mater. Charact. 171 (2021), 110822.
[52] O. El-Atwani, W.S. Cunningham, D. Perez, E. Martinez, J.R. Trelewicz, M. Li, S. A. Maloy, Scr. Mater. 180 (2020) 6–10.
[53] F.I. Allen, Beilstein J. Nanotechnol. 12 (2021) 633–664.
[54] J.F. Ziegler, J.P. Biersack. Stopping Range of Ions in Matter, 1985.
[55] T. Kurki-Suonio, O. Asunta, T. Hellsten, V. Hynönen, T. Johnson, T. Koskela, J. Lönnroth, V. Parail, M. Roccella, G. Saibene, A. Salmi, S. Sipilä, Nucl. Fusion 49 (2009).
[56] A.Y. Konobeyev, U. Fischer, Y.A. Korovin, S.P. Simakov, Nucl. Energy Technol. 3 (2017) 169–175.
[57] M.J. Banisalman, S. Park, T. Oda, J. Nucl. Mater. 495 (2017) 277–284.
[58] Y. Yang, D. Frazer, M. Balooch, P. Hosemann, J. Nucl. Mater. 512 (2018) 137–143.
[59] D. Kiener, A.M. Minor, O. Anderoglu, Y. Wang, S.A. Maloy, P. Hosemann, J. Mater. Res. 27 (2012) 2724–2736.
[60] P. Hosemann, C. Shin, D. Kiener, J. Mater. Res. 30 (2015) 1231–1245.
[61] C. Bonnekoh, U. Jäntsch, J. Hoffmann, H. Leiste, A. Hartmaier, D. Weygand, A. Hoffmann, J. Reiser, Int. J. Refract. Met. Hard Mater. 78 (2019) 146–163.